Self-Aligned Inkjet Printing of Resistors and Low-Pass *RC* Filters on Roll-to-Roll Imprinted Plastics with Resistances Ranging from 10 to 10^6 Ω

Motao Cao, Krystopher Jochem, Woo Jin Hyun, Lorraine F. Francis and

C. Daniel Frisbie

Department of Chemical Engineering and Materials Science, University of Minnesota, 421 Washington Avenue S.E., Minneapolis, Minnesota 55455, United States

E-mail: frisbie@umn.edu, lfrancis@umn.edu

Received xxxxxx
Accepted for publication xxxxxx
Published xxxxxx

Abstract

Resistors are essential and ubiquitous building blocks in electronic circuits. Fabrication of printed resistors in a manner compatible with roll-to-roll printing is important for realizing low-cost and high-throughput production of electronic devices. Here we present fully printed resistors fabricated via a novel self-aligned printing method termed SCALE (Self-aligned Capillarity Assisted Lithography for Electronics). Flexible substrates with imprinted features such as reservoirs and capillary channels were prepared by roll-to-roll processing. Functional inks were then delivered sequentially into the reservoirs by inkjet printing and the ink flowed spontaneously into the adjoining channels driven by capillarity. Poly(3,4-ethylene dioxythiophene):poly(styrene sulfonate) (PEDOT:PSS) was used as the resistive material, and silver was used for the electrodes. Using SCALE, we achieved fully inkjet-printed, self-aligned resistors with resistance values ranging over five orders of magnitude while keeping the overall dimensions of the devices constant. We then employed SCALE to build low-pass *RC* (resistor-capacitor) filters with cutoff frequency from 0.4 - 27 kHz and excellent operational stability. Overall, this work expands the potential of self-aligned inkjet printing for producing fully printed electronic circuits.

Keywords: resistors, inkjet printing, PEDOT:PSS, *RC* filter, flexible electronics

1. Introduction

The use of printing strategies for production of flexible circuits on plastic or paper substrates is attractive for several reasons including the compatibility of printing with continuous, roll-to-roll processing, scalability to large areas at lower cost, and reduced materials waste by eliminating subtractive etching steps [1]. Printed and flexible circuits have potential applications in large area sensor arrays [2], wearable electronics [3], displays [4], smart labels [5], and medical diagnostics [6, 7]. Among printing techniques, inkjet printing has been widely used for printed electronics demonstrations due to its numerous advantages including digital control, non-contact operation, materials compatibility, minimal material waste, and widespread commercial acceptance [8-22]. However, its application in high-throughput roll-to-roll processing of multilayered microelectronic circuits is limited currently by poor resolution and materials registration challenges.

To solve this problem, a novel inkjet-based printing method called self-aligned capillarity-assisted lithography for electronics (SCALE) has been developed [23]. The SCALE process starts with imprinting a multi-level network of open reservoirs, capillaries, and device cavities in a UV curable coating on a flexible substrate. Subsequent materials deposition and layer-to-layer alignment is achieved by

inkjetting electronic inks sequentially into the easy-to-hit reservoirs, followed by spontaneous capillary flow of the inks via open channels into cavities shaping discrete electronic components. The SCALE process thus combines imprint lithography with inkjet printing to enhance printed resolution - linewidths of 1 μm are readily achievable - while simultaneously simplifying materials registration. An additional benefit of SCALE is that crisp, well-defined line edges characteristic of conventionally photopatterned materials are readily obtainable, which is not typical of inkjet printing [24, 25].

Already, successful fabrication of discrete circuit elements including transistors, capacitors, and resistors on individual plastic sheets has been demonstrated by SCALE [23, 26-30]. However, the use of SCALE and roll-to-roll processing to create resistors with resistances over many orders of magnitude has not been demonstrated. As resistors are ubiquitous electronic building blocks, this is a crucial challenge for the ultimate goal of roll-to-roll printing of complete circuits. Indeed, printed resistors have been realized utilizing screen printing [31-34], stencil printing [35], aerosol jet printing [36] and inkjet printing [24, 37-39], but these fabrication procedures were not completely compatible with self-alignment and/or roll-to-roll processing. Thus, in this paper we focus on demonstrating SCALE-based, roll-to-roll approaches to creating resistors with resistances spanning many orders of magnitude.

Key to this effort is the choice of printable resistive materials. Poly(3,4-ethylene dioxythiophene):poly(styrene sulfonate) (PEDOT:PSS), which has been widely used as both a conductive and a resistive material in printed electronics, is an ideal material due to its adjustable resistivity and good printability. It has been reported that the resistivity of PEDOT:PSS films deposited from the commercial PH1000 ink (Heraeus) can be decreased by adding a small amount of high boiling point solvents such as dimethyl sulfoxide (DMSO) and ethylene glycol (EG) [40, 41]. Jung, et al. reported inkjet-printed resistors using PEDOT:PSS PH1000 inks [24]. They modified the film resistivity by varying the concentration of DMSO added into the solution. Also, Ali et al. increased the resistivity of PEDOT:PSS films from 48 to 210 mΩ·cm by blending poly(methyl methacrylate)(PMMA) into PH1000 PEDOT:PSS ink [25]. Though not explored here, carbon based inks can also be used to print the resistive layer. Chang, et al. blended high (Dupont 5036) and low (Dupont 7082) resistivity carbon materials and achieved a resistance range from 3.3 kΩ/□ to 800 kΩ/□ using screen printing [32].

In order to make resistors having resistance ranging over orders of magnitude, but with the same spatial footprint, which is important for circuit layout considerations, we employed a two-pronged strategy in which the distance between printed electrodes was changed in concert with alterations of the PEDOT:PSS ink formulation to adjust resistivity, as just described. We achieved resistors on plastic substrates with resistances varying from 10-10^6 Ω. The resistors were robust to bending strains of up to 1% and to thousands of repeated electrical measurements. To test dynamic performance, we printed low-pass *RC* (resistor-capacitor) filters. The fabrication of *RC* filters by inkjet printing was first reported by Varahramyan and colleagues [42-44]. Then, Castro, et al. demonstrated all-inkjet-printed low-pass filters with cutoff frequency from 82 Hz to 740 Hz by applying printed organic thin-film transistors [45]. Here we demonstrate fully printed low-pass *RC* filters with cutoff frequencies over three orders of magnitude by varying the resistance. Collectively, the results demonstrate that the SCALE process has excellent potential for self-aligned printing of resistors and *RC* filters necessary for building more advanced electronic systems on flexible substrates.

2. Experimental Section

2.1 Silicon master template fabrication

The silicon master template was fabricated by two rounds of traditional photolithography. (a) Patterning the recessed reservoirs and channels for electrodes: A 4-in silicon wafer was heated at 115 ºC for 1 min to remove the water molecules on the top surface. Then the wafer was treated in a hexamethyldisilazane (HMDS) atmosphere for 4 min. A layer of photoresist (Microposit S1813, Dow) was spin-coated onto the silicon wafer at 3000 rpm for 30 s. The wafer was soft-baked at 115 ºC for 1 min and then exposed to UV light for 5 s under a photomask designed for the electrodes. The wafer was developed in a mixture of Microposit 351 (Dow) and deionized water (1:5 v/v) for 30 s. The exposed area of the wafer was dry etched down to a depth of 7 μm in a deep trench etcher (SLR 770). The photoresist was then washed off by acetone and the wafer was immersed in Piranha solution (H_2SO_4 and H_2O_2, 1:1) for 20 min at 120 ºC to clean the residual photoresist. (b) Patterning the raised ink receivers: SU-8 2010 photoresist (MicroChem) was spin-coated onto the same silicon wafer at 500 rpm for 5 s and then at 2000 rpm for 30 s, followed by baking at 65 ºC for 3 min and 95 ºC for 7 min. The photoresist was then exposed to UV light for 24 s through the photomask designed for the raised walls. The exposed wafer was heated at 65 ºC for 1 min and 95 ºC for 7 min. The wafer was immersed in 1-methoxy-2-propanyl acetate for 5 min to develop the photoresist and then rinsed with isopropyl alcohol. Lastly, the wafer was baked at 180 ºC for 10 min.

2.2 PDMS Stamp Fabrication

The silicon master template was first silane-treated in a vacuum chamber overnight with trichloro(1H,1H,2H,2H-perfluorooctyl)silane (Aldrich). A curing agent and PDMS

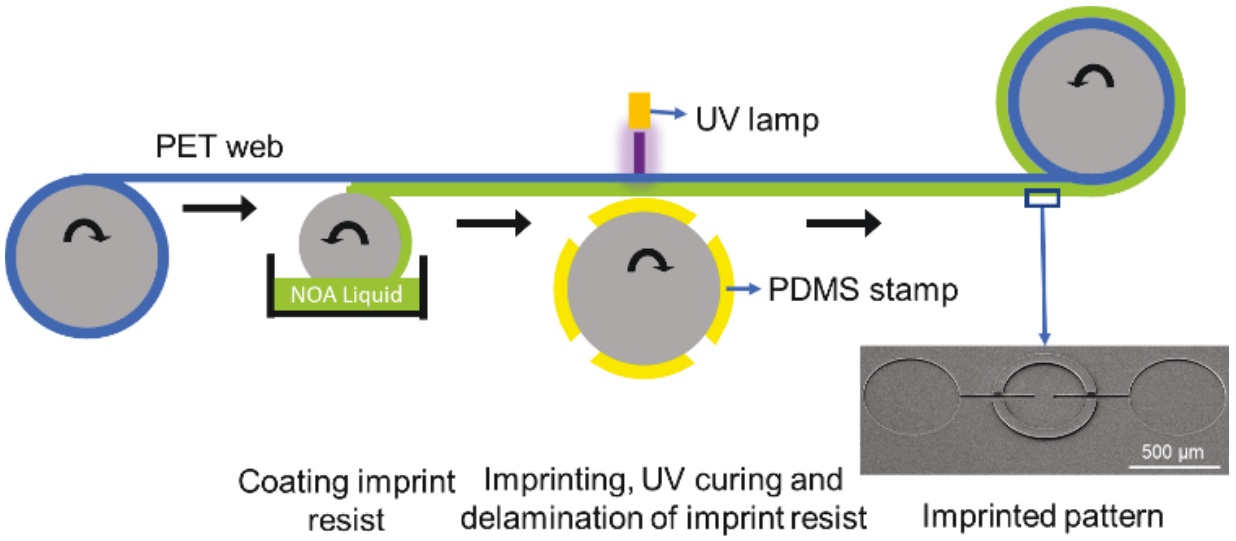

Figure 1. Schematic illustration of roll-to-roll imprinting of reservoirs, capillary channels, and device cavities for the SCALE process. The imprint material (green) is a cross-linkable liquid that is cured by UV illumination while the web is in contact with the PDMS stamp roll, as shown.

monomer (Sylgard 184, Dow Corning) were mixed in a weight ratio of 1:10 and then poured onto the silicon master template. The PDMS was first cured at 70 ºC for 2 h in an oven. Then the PDMS stamp was peeled off from the silicon wafer, followed by heating at 120 ºC for 2 h and at 215 ºC for another 2 h to enhance the mechanical durability.

2.3 Roll to Roll Imprinting of the Flexible Substrates

The imprinting of the flexible substrates was performed on a roll-to-roll machine (Carpe Diem Technologies). The PDMS stamps were glued to a piece of silicone coated PET sheet and cured at 45 ºC for 1 day. The PET sheet with the PDMS stamps on it was then wrapped around the imprinting drum and clamped in place. A pre-cleaned PET web, which was used as the flexible substrate, was coated with a liquid layer of UV-curable imprint resist (Norland Optical Adhesive 73, Norland Products) to a thickness of 25 µm by reverse gravure coating. The web then passed at 10 cm/min and 18 N web tension to the imprint drum where the PDMS molds were pressed into the NOA layer. A high intensity UV light cured the resist coating while it was still in contact with the stamp. The web with the imprinted layer was then delaminated from the PDMS stamp roll and spooled up.

2.4 Ink Preparation

The resistive inks were prepared following the compositions listed in Table 1. Two types of PEDOT:PSS inks (Clevios PH1000 and Clevios AI4083) were purchased from Heraeus. Ethylene glycol was purchased from Sigma Aldrich. Isopropyl alcohol (10 vol%) was added to reduce the surface tension. The inks were sonicated for 15 min and filtered through a 5 µm pore filter before each use. The ion-gel ink was prepared by mixing an ionic liquid (1-ethyl-3-methylimidazolium bis(trifluoromethylsulfonyl)imide, [EMIM][TFSI]), a triblock copolymer (poly (styrene-b-ethyl acrylate-b-styrene), SEAS) and *n*-butyl acetate to a weight ratio of 8:2:90.

2.5 Device Fabrication

For printing the resistor, a reactive silver ink [26] was delivered into the electrode reservoirs by inkjet printing followed by a 3-min annealing process at 100 ºC in air to generate the two electrodes. Then the PEDOT:PSS ink was also inkjet-printed into the round ink receiver in the center of the device to cover the gap between the two electrodes followed by drying at 100 ºC in air for 10 min, resulting in a 1-µm thick PEDOT:PSS film. For printing the *RC* filter, the interdigitated electrodes and the connection wires were also printed from the reactive silver ink. Then the PEDOT:PSS ink and the ion-gel ink were delivered respectively into their raised receivers and were annealed at 100 ºC for 10 min in air together. A piezoelectric nozzle (Microfab) with an orifice of 80 µm was used for the inkjet printing. A unipolar waveform was applied during the jetting with a rise time of 5 µs, a dwell time of 20 µs, a down time of 5 µs, a driving voltage of 120 V and a frequency of 1000 Hz. 8 nL of the silver ink (20 drops) was delivered into each of the electrode reservoir and 27 nL of the PEDOT:PSS ink (70 drops) was delivered into the corresponding ink receiver.

2.5 Characterization

The optical images of the devices were taken by an optical microscope (Keyence). Film thickness profiles were measured by a Tencor P-7 profilometer. The surface tensions were measured by a pendant drop shape analyzer (Kruss). The resistivities of the PEDOT:PSS films were measured via the

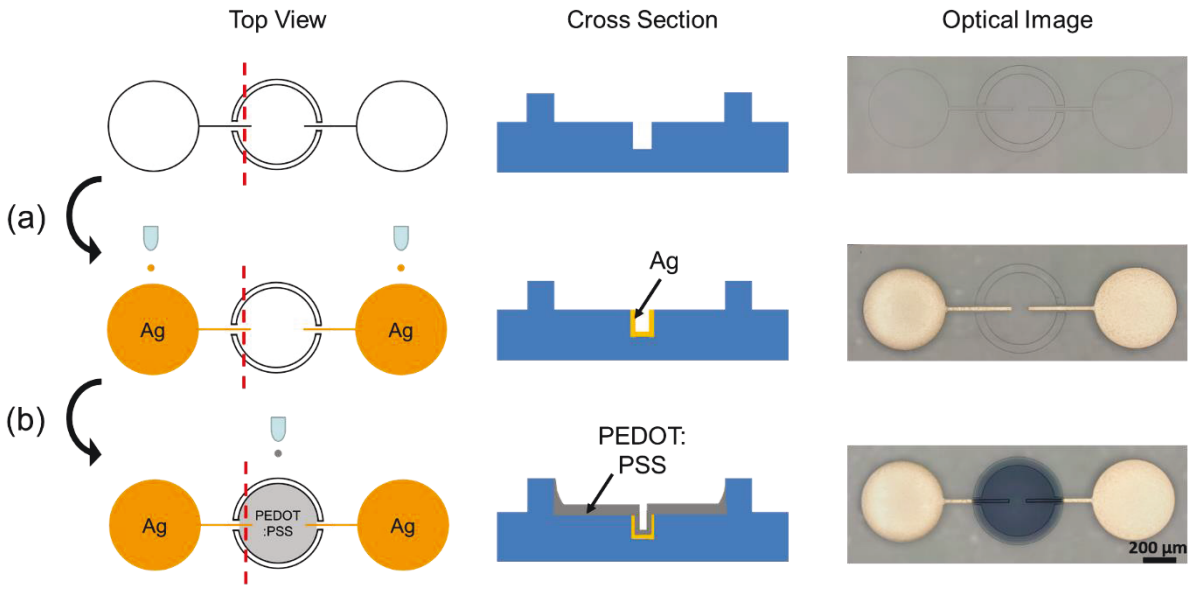

Figure 2. Top-view (left) and cross-sectional (middle) illustrations and optical images (right) for the fabrication of a resistor via the SCALE process. The cross-sectional illustrations show the topographic profile along the red dashed lines in the top-view illustrations. (a) When the silver ink is delivered to the reservoirs by inkjet printing, the ink is patterned into the channels by capillary action and forms electrodes after thermal annealing. (b) PEDOT:PSS ink is delivered to the center ink receiver to form a resistive layer between the electrodes.

Van der Pauw method on spin-coated PEDOT:PSS films on square glass slides. To calculate the resistance, current-voltage curves were measured under a N_2 atmosphere using two source meters (Keithley 236 and 237). For the electrical characterization of the *RC* filter, the input signals were generated by a waveform generator (Agilent 33512B). The output voltages were acquired with a digital oscilloscope (Tektronix TDS3014C). The capacitance of the printed ion-gel capacitor was measured by an impedance analyzer (HP4192A LF).

3. Results and discussion

Figure 1 illustrates the roll-to-roll process to prepare the imprinted substrates for resistors. Prior to the roll-to-roll imprinting process, a silicon master template (Figure S1a) was prepared by traditional photolithography methods, and the patterns were transferred to PDMS stamps (Figure S1b, c). The PDMS stamps were secured around an imprinting drum in the roll-to-roll machine. When the PET web, which was pre-coated with a layer of UV curable imprint resist, passed through the imprinting drum at a speed of 10 cm/min, the PDMS stamps were pressed into the imprint coating to create the capillary channels and connected reservoirs. At the same time, the imprint layer was cured by a high intensity UV light. The imprinted web was peeled off from the PDMS stamps and collected by a rewind drum. The channels (20 µm wide and 7 µm deep), reservoirs (500 µm in diameter and 7 µm deep) and ink receivers (500 µm in diameter and 10 µm above the plane) were successfully replicated onto flexible substrates from the silicon master template, which is shown by the tilted scanning electron microscopy (SEM) image in Figure 1. Compared with our previous SCALE resistor design [23], this new design reduced the device area from 2.8 mm^2 to 1.0 mm^2. Further reductions should be possible in future designs with smaller reservoirs.

Figure 2 shows the printing steps of a resistor on the imprinted substrate. To generate electrodes (Figure 2a), a particle free silver ink [46] was delivered into the two reservoirs on both sides by inkjet printing. The silver ink wicked into the capillary channels, and then formed conductive silver films in the channels connected to the reservoirs upon annealing. Compared with directly writing the electrodes by conventional inkjet printing, the SCALE process (1) increased resolution by preventing lateral spreading of the silver ink, (2) provided straight electrodes with highly smooth edges, and (3) simplified registration of the two electrodes with respect to each other, i.e., precise nozzle alignment was not required to produce the two electrodes with the desired spacing and co-linear alignment. To deposit the resistor layer and complete the device, PEDOT:PSS ink was delivered into the center ink receiver, bridging the two electrodes (Figure 2b).

To manipulate the total electrical resistance (R) of the device, the resistive film was deposited using a mixture of two types of PEDOT:PSS solutions (purchased from Heraeus) with different intrinsic resistivities: PH1000 (resistivity: 1.3 Ω·cm) and AI4083 (resistivity: 8800 Ω·cm). Figure 3a shows the PEDOT:PSS film resistivity measured in Van der Pauw geometry as a function of the mixing ratio of the two inks. The film resistivity increases with the concentration of AI4083 and

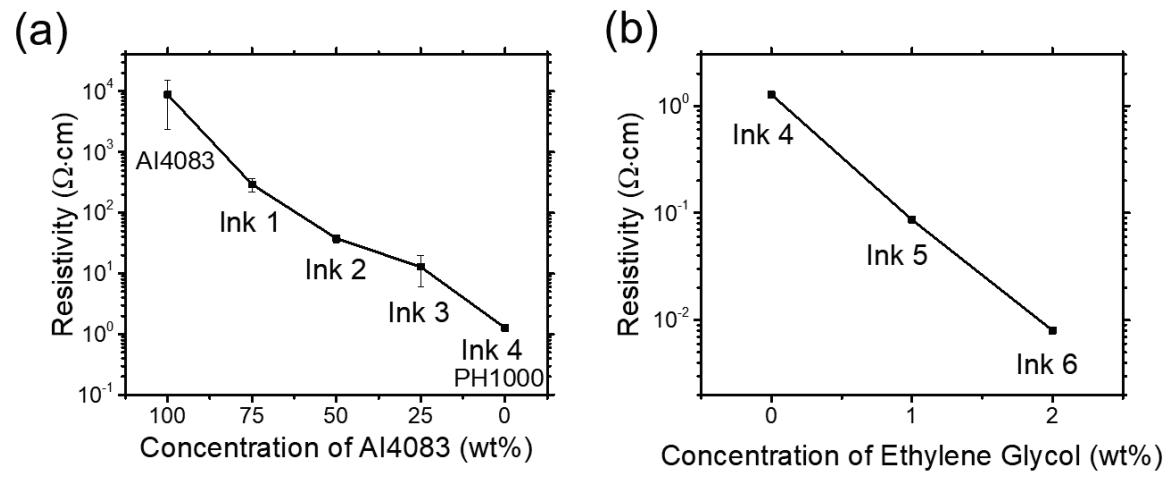

Figure 3. (a) Resistivity of PEDOT:PSS films printed from a mixture of PH1000 and AI4083 for different mixing ratios. Error bars represent one standard deviation. (b) Resistivity of PEDOT:PSS films versus the weight fraction of ethylene glycol in the PH1000 ink. Note that the error bars (one standard deviation) are not visible in this panel as they are smaller than the data points.

can be controlled in a wide range from 1 to 300 Ω·cm by the mixing ratio. Moreover, the resistivity can be further adjusted by the addition of ethylene glycol (EG) into the PH1000 solution. It is proposed in the literature that the addition of ethylene glycol induces a conformational change of the PEDOT chains from coiled to linear or to an expanded-coil conformation [41, 47]. This change leads to enhanced charge carrier transport within the PEDOT:PSS film and results in a lower resistivity. As shown in Figure 3b, the resistivity of the PEDOT:PSS film printed from the PH1000 ink decreases from 1 to 0.008 Ω·cm with the addition of only 2 wt% of ethylene glycol. Therefore, the resistivity of the printed PEDOT:PSS film can be changed over five orders of magnitude by simply modifying the ink formulation.

Table 1. Composition of PEDOT:PSS ink formulations

Ink #	PH1000 (wt%)	AI4083 (wt%)	Ethylene glycol (wt%)
Ink 1	25	75	0
Ink 2	50	50	0
Ink 3	75	25	0
Ink 4	100	0	0
Ink 5	99	0	1
Ink 6	98	0	2

All inks were modified with 10 vol% isopropyl alcohol.

In addition to controlling the electrical resistivity, another way to manipulate the device resistance is controlling the distance between the two electrodes. For facile control of the resistance with the electrode separation *L* (Figure 4a), the film uniformity is important because a linear relationship between the resistance and the electrode separation can be expected when the film thickness is uniform in the center ink receiver. However, the resistive layer printed using the as-received PEDOT:PSS solution shows significant thickness variation, as evident in the profile (Figure 4b). To improve the thickness uniformity, isopropyl alcohol (IPA) was added to the PEDOT:PSS solutions to reduce the surface tension of the inks. As previously reported, Xing, et.al. suggested that the addition of IPA into the PEDOT:PSS inks led to a film with a flatter top surface in a confined groove due to a reduction in the ink surface tension [48]. The surface tension of PH1000 was measured without and with IPA, as shown in Figure 4c. The surface tension of the ink decreases with the IPA content because IPA has a much lower intrinsic surface tension (23 mN/m) than the aqueous PH1000 ink (68.5 mN/m). As a result, the PEDOT:PSS film exhibits significantly improved thickness uniformity after the addition of IPA to the ink (Figure 4d) while the film resistivity remains almost unchanged (Figure 4c).

The relationship between the resistance and the electrode separation (*L*) was explored for various resistance ranges by employing different PEDOT:PSS ink formulations (Table 1) modified with IPA (10 vol% in the inks). Figures 5 a-f display the plots of the resistance as a function of *L* for devices fabricated with different inks. Each data point represents the average and the standard deviation for 20 devices, and 600 devices in total were fabricated with a yield of 100%. The standard deviations of resistance were all less than 15% and could be further reduced upon optimization of the printing precision to achieve better thickness control of the PEDOT:PSS film. The results demonstrate that the resistance increases linearly with the electrode separation and the linear relationship holds well for all the resistance ranges with R^2 higher than 0.9. Typical current-voltage curves of printed

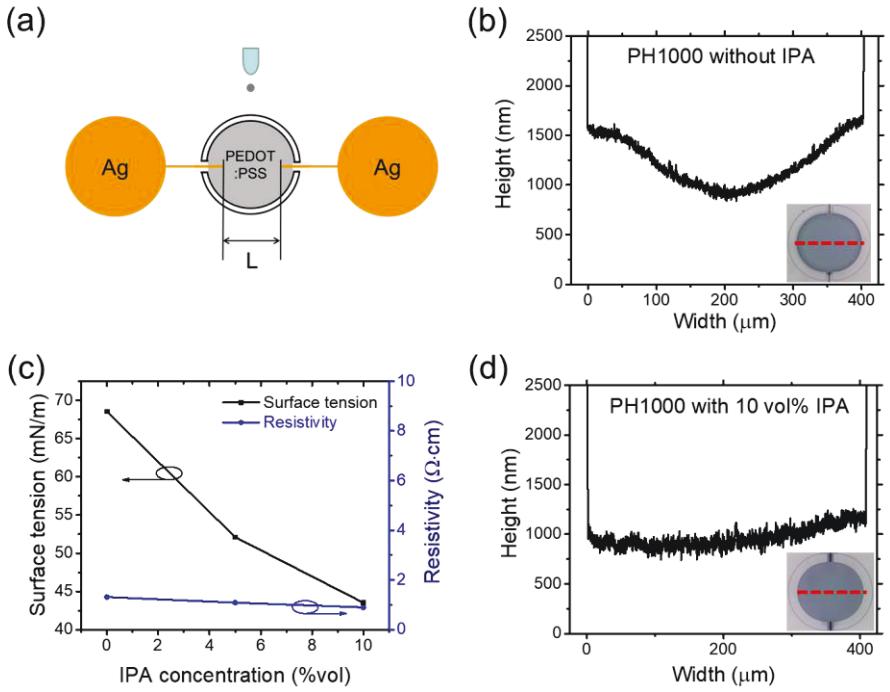

Figure 4. (a) Sketch defining the electrode separation L. (b) Thickness profile of the PEDOT:PSS film (in the ink receiver) printed using (b) as-received PH1000 and (d) a mixture of PH1000 and isopropanol (9:1 vol/vol). The profiles were taken along the red dashed lines shown in the inset optical images. (c) Surface tension of PH1000 inks blended with isopropyl alcohol and resistivity of PEDOT:PSS films printed using these inks.

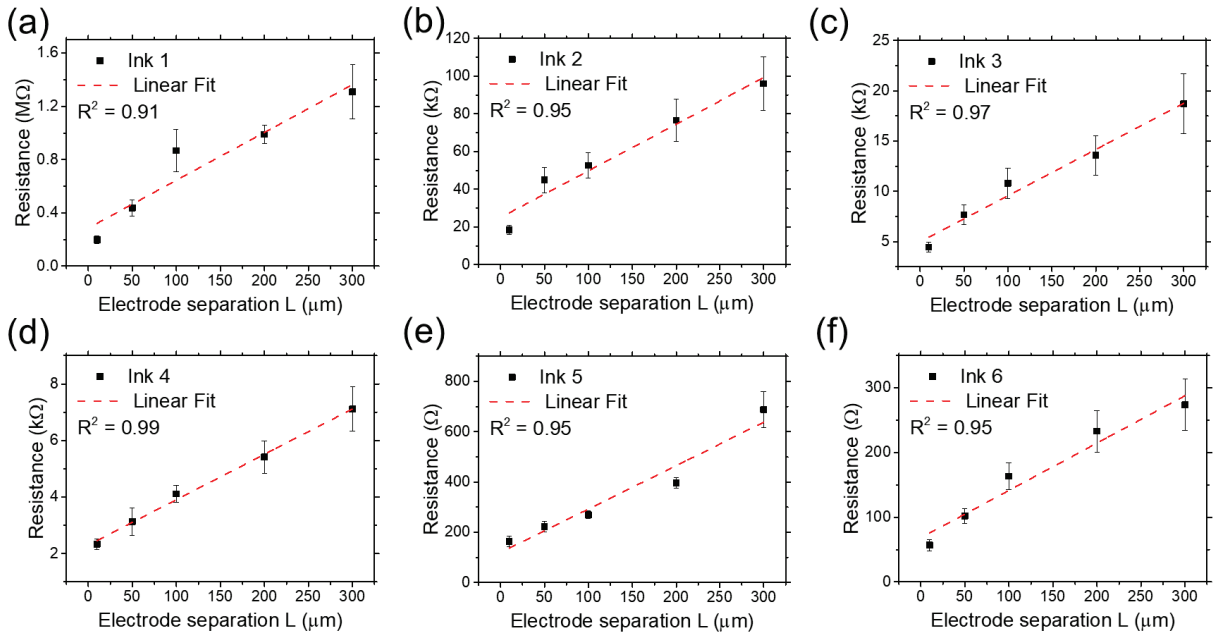

Figure 5. (a)-(f) Resistance as a function of L for resistors printed with different ink formulations (see Table 1). The red dashed line shows the linear fit of the five data points in each figure.

resistors covering all the resistance ranges indicate good linear response (Figure S2). We found that the resistors could withstand a maximum current of 5 mA. Finally, a resistance range over five orders of magnitude from 57 Ω to 1.3 MΩ was achieved with good repeatability.

To investigate the mechanical flexibility of the printed resistors (Figure 6a), a bending test (Figure 6b) was performed with a bending radius of 1 cm (tensile strain of about 0.8%). The device resistance was monitored during the bending test and did not exhibit a significant change over 5000 bending

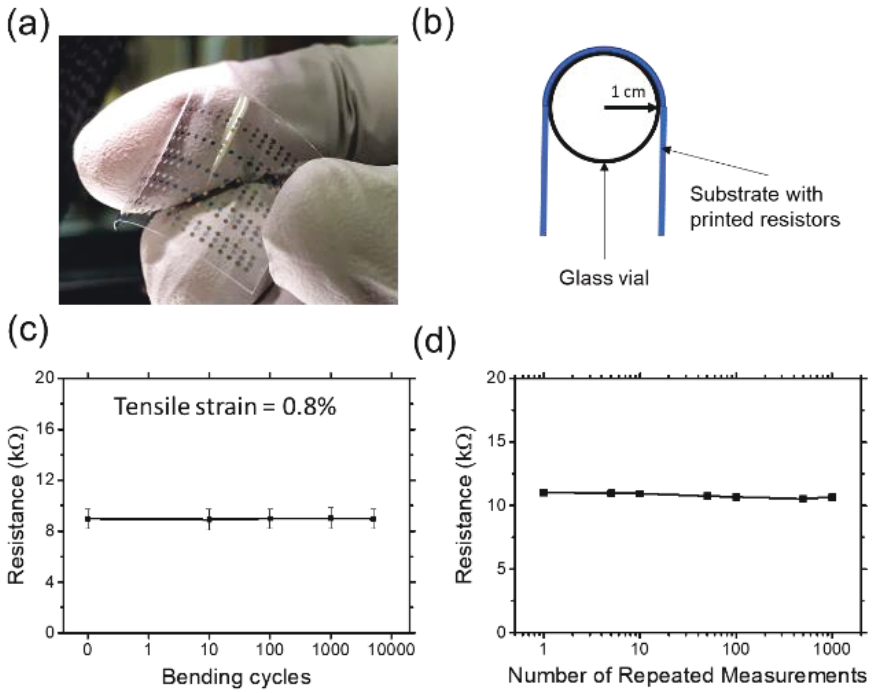

Figure 6. (a) Photograph of a 20 × 5 array of printed resistors on a PET substrate. (b) A schematic drawing of the bending test along the length of the resistors with a bending radius of 1 cm. (c) The resistance changes with bending cycles for the printed resistors. The averages and the standard deviations show the results collected from 5 devices. (d) The resistance changes with the number of repeated IV measurements of one device.

cycles, as shown in Figure 6c, revealing excellent tolerance to bending. Moreover, the operational stability was examined by acquiring standard current-voltage curves of the resistors repeatedly. The resistance values are plotted against the number of measurements in Figure 6d. Typical resistors retained over 96% of their original resistance after 1000 measurements, showing good long-term operational stability.

To examine dynamic behavior, low-pass *RC* filters employing the printed resistors (Figure 7a) were demonstrated. The capacitor of the *RC* filter was also fabricated via the SCALE process using a previously reported procedure [27]. The underlying silver electrodes are in a co-planar interdigitated structure with six digits in total. A gel electrolyte composed of an ionic liquid [EMIM]:[TFSI] and a copolymer (see experimental), was employed as the dielectric material due to its high specific capacitance, excellent printability at room temperature, and good mechanical integrity [49, 50]. The capacitance of an individual printed capacitor is shown as a function of frequency in Figure S3. The maximum operating voltage is approximately 3V. Figure 7b shows an optical image of a completed *RC* filter.

The transient response of the *RC* filter was measured by applying a square wave input signal and collecting the output signal using a digital oscilloscope. Figures 7 c-f show the transient responses of the *RC* filter consisting of a 90 kΩ resistor and a 0.45 nF capacitor at different frequencies. For an ideal low-pass *RC* filter, the output voltage within the time domain can be predicted by

$$V_{out} = V_{in}\left(1 - e^{-\frac{t}{RC}}\right) \quad (1)$$

where V_{in}, R, C, and t are the input voltage, resistance, capacitance, and time, respectively [51]. RC is the time constant, which is 40.5 μs in this case. When the RC constant is much smaller than the period of the input signal, that is, at a low frequency (f = 10 Hz, Figure 7c), the waveform of the output signal matches the input signal very well and $V_{out} \approx V_{in}$. The output signal follows the input signal well up to 1 kHz (Figure 7d). At 5 kHz, the period of the input signal is small enough to be comparable to the RC constant, so the amplitude of the output voltage starts to diminish (Figure 7e). When the frequency is further increased, the amplitude of the output voltage drops significantly until no output waveform is observed at 1 MHz (Figure 7f). The results show that the dependence of the transient responses on the input frequency is in good agreement with the theoretical prediction, indicating that printed low-pass *RC* filters via the SCALE process are fully functional and rationally designed. In addition, an operational stability test was performed on the *RC* filter. As shown in Figure 7g, the transient response of the device shows negligible change after 12 h of continuous operation at a frequency of 1 kHz under inert atmosphere, indicating good long-term operational stability.

To demonstrate the tunability of the cutoff frequency, low-pass *RC* filters were fabricated using resistors with different resistances (12, 90, 800 kΩ), as shown in Figure 7h. A low-

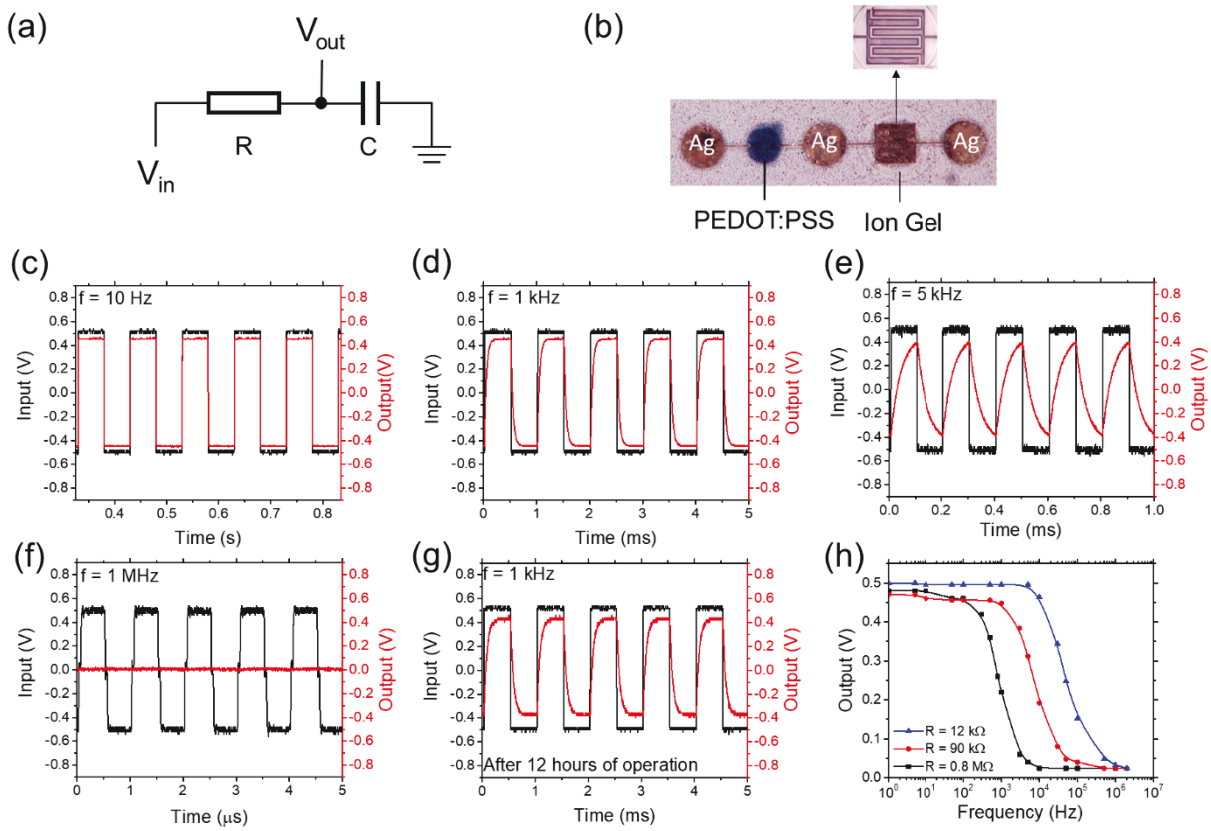

Figure 7. (a) Equivalent circuit of the printed low-pass RC filters. (b) Optical image of a completed RC filter with a PEDOT:PSS resistor and an ion-gel capacitor. Transient response of a RC filter with a resistor of 90 kΩ under a square wave input at frequencies of (c) 10 Hz, (d) 1 kHz, (e) 5 kHz, (f) 1 MHz, and (g) 1 kHz after 12 hours of continuous operation. (h) Frequency response of printed low-pass RC filters with resistors of 0.8 MΩ, 90 kΩ and 12 kΩ.

pass *RC* filter allows signals with frequencies below the cutoff frequency to pass through with little to no attenuation, while suppressing or blocking the ones with higher frequencies. The cut-off frequency is defined as

$$f_c = \frac{1}{2\pi RC} \quad (2)$$

at which the amplitude of the output voltage is reduced to $V_{out} = V_{in}/\sqrt{2}$ [51]. The theoretical cutoff frequencies are compared with the experimental cutoff frequencies estimated from the frequency response curves (Figure 7h), as summarized in Table 2. The results show that the measured cutoff frequencies agree well with the calculated cutoff frequencies, demonstrating that varying the resistance is a reliable way to tailor the cutoff frequency of the printed low-pass *RC* filter. The cutoff frequency can be adjusted over two orders of magnitude from 400 Hz to 27 kHz simply by changing the resistance.

Table 2. Experimentally estimated and theoretically calculated cut-off frequencies of the printed *RC* filters

Resistance	Capacitance	Cut-off frequency from experiments	Cut-off frequency calculated theoretically
12 kΩ	5.00×10^{-10} F	26.8 kHz	26.5 kHz
90 kΩ	4.54×10^{-10} F	4.3 kHz	3.9 kHz
0.8 MΩ	4.59×10^{-10} F	477 Hz	434 Hz

4. Conclusion

In this work, we demonstrated self-aligned inkjet printed resistors on roll-to-roll imprinted flexible substrates with resistances ranging over five orders of magnitude. Changes in resistance within one order of magnitude were achieved by varying the separation of the two electrodes, while larger changes were made by blending the PEDOT:PSS PH1000 ink with ethylene glycol or PEDOT:PSS AI4083 ink. A linear relationship was observed between the resistance and the electrode separation, indicating precise control of the resistance. The printed flexible resistors exhibited high mechanical durability and outstanding operational stability. Inkjet-printed low pass RC filters with predictable and stable dynamic performance were also successfully fabricated using the SCALE process. The cut-off frequency was varied over two orders of magnitude by simply changing the resistance of the resistor. The SCALE method appears to be a promising way to facilitate the fabrication of flexible resistors by roll-to-

roll processing. Future work will focus on shrinking the size of the reservoirs to further reduce the footprint and integrating the resistors into flexible circuits.

Acknowledgements

The authors thank two undergraduate students Yuheng Miao and Alayna Erickson for their help in completing this project. This work was supported by the Multi-University Research Initiative (MURI) program sponsored by the Office of Naval Research (MURI Award N00014-11-1-0690). Additional support was provided by the National Science Foundation (NSF) under grant number CMMI-1634263 and the Xerox Research Centre of Canada. Krystopher Jochem further acknowledges support from the National Science Foundation Graduate Research Fellowship Program under Grant No. 00039202. The authors thank Prof. Jennifer Lewis (Harvard University) and Dr. Brett Walker (Electroninks, Inc.) for providing silver ink and for collaboration on the use of the ink in SCALE. Parts of this work were carried out at the Characterization Facility, University of Minnesota, which receives partial support from NSF through the MRSEC program. Portions of this work were conducted in the Minnesota Nano Center, which is supported by the National Science Foundation through the National Nano Coordinated Infrastructure Network (NNCI) under Award Number ECCS-1542202.

References

[1] Ivanova O, Williams C and Campbell T 2013 *Rapid Prototyping. J.* **19** 353-64
[2] Yao S and Zhu Y 2014 *Nanoscale* **6** 2345-52
[3] Wataru H, Shingo H, Takayuki A, Seiji A and Kuniharu T 2014 *Adv. Funct. Mater.* **24** 3299-304
[4] Street R A, Wong W S, Ready S E, Chabinyc M L, Arias A C, Limb S, Salleo A and Lujan R 2006 *Mater. Today* **9** 32-7
[5] Street R A, Ng T N, Schwartz D E, Whiting G L, Lu J P, Bringans R D and Veres J 2015 *Proc. IEEE* **103** 607-18
[6] Yeo W H, Kim Y S, Lee J, Ameen A, Shi L, Li M, Wang S, Ma R, Jin S H, Kang Z, Huang Y and Rogers J A 2013 *Adv. Mater.* **25** 2773-8
[7] Corea J R, Lechene P B, Lustig M and Arias A C 2017 *Magn. Reson. Med.* **78** 775-83
[8] Calvert P 2001 *Chem. Mater.* **13** 3299-305
[9] Gans B J D, Duineveld P C and Schubert U S 2004 *Adv. Mater.* **16** 203-13
[10]Scheideler W J, Kumar R, Zeumault A R and Subramanian V 2017 *Adv. Funct. Mater.* **27** 1606062
[11]Ng T N, Schwartz D E, Mei P, Kor S, Veres J, Bröms P and Karlsson C 2015 *Flexible and Printed Electronics* **1** 015002
[12]Bucella S G, Salazar‐Rios J M, Derenskyi V, Fritsch M, Scherf U, Loi M A and Caironi M 2016 *Adv. Electron. Mater.* **2** 1600094
[13]Sirringhaus H, Kawase T, Friend R H, Shimoda T, Inbasekaran M, Wu W and Woo E P 2000 *Science* **290** 2123-6
[14]Ng T N, Wong W S, Chabinyc M L, Sambandan S and Street R A 2008 *Appl. Phys. Lett.* **92** 213303
[15]Kawase T, Sirringhaus H, Friend R H and Shimoda T 2001 *Adv. Mater.* **13** 1601-5
[16]Ng T N, Mei P, Schwartz D E, Kor S, Krusor B, Veres J, Bröms P, Eriksson T, Wang Y, Hagel O and Karlsson C 2015 *SPIE Organic Photonics + Electronics* **9569** 6
[17]Tobjörk D, Kaihovirta N J, Mäkelä T, Pettersson F S and Österbacka R 2008 *Org. Electron.* **9** 931-5
[18]Khan Y, Pavinatto F J, Lin M C, Liao A, Swisher S L, Mann K, Subramanian V, Maharbiz M M and Arias A C 2016 *Adv. Funct. Mater.* **26** 1004-13
[19]Whiting G L and Arias A C 2009 *Appl. Phys. Lett.* **95** 253302
[20]Lessing J, Glavan A C, Walker S B, Keplinger C, Lewis J A and Whitesides G M 2014 *Adv. Mater.* **26** 4677-82
[21]Zirkl M, Sawatdee A, Helbig U, Krause M, Scheipl G, Kraker E, Ersman P A, Nilsson D, Platt D, Bodö P, Bauer S, Domann G and Stadlober B 2011 *Adv. Mater.* **23** 2069-74
[22]Homenick C M, James R, Lopinski G P, Dunford J, Sun J, Park H, Jung Y, Cho G and Malenfant P R L 2016 *ACS Appl. Mater. Interfaces* **8** 27900-10
[23]Mahajan A, Hyun W J, Walker S B, Rojas G A, Choi J H, Lewis J A, Francis L F and Frisbie C D 2015 *Adv. Electron. Mater.* **1**
[24]Jung S, Sou A, Gili E and Sirringhaus H 2013 *Org. Electron.* **14** 699-702
[25]Ali S, Bae J and Lee C H 2015 *Appl. Phys. A* **119** 1499-506
[26]Hyun W J, Bidoky F Z, Walker S B, Lewis J A, Francis L F and Frisbie C D 2016 *Adv. Electron. Mater.* **2**
[27]Hyun W J, Secor E B, Kim C H, Hersam M C, Francis L F and Frisbie C D 2017 *Adv. Energy Mater.*
[28]Mahajan A, Hyun W J, Walker S B, Lewis J A, Francis L F and Frisbie C D 2015 *ACS Appl. Mater. Interfaces* **7** 1841-7
[29]Song D, Bidoky F Z, Hyun W J, Walker S B, Lewis J A and Frisbie C D 2018 *ACS Appl. Mater. Interfaces* **10** 15926-32
[30]Woo Jin H, Ethan B S, Fazel Zare B, Walker S B, Jennifer A L, Mark C H, Lorraine F F and Frisbie C D 2018 *Flexible and Printed Electronics* **3** 035004
[31]Numakura D 2008 *2008 3rd International Microsystems, Packaging, Assembly & Circuits Technology Conference* 205-8
[32]Chang J, Zhang X, Ge T and Zhou J 2014 *Org. Electron.* **15** 701-10
[33]Słoma M, Jakubowska M, Kolek A, Mleczko K, Ptak P, Stadler A W, Zawiślak Z and Młożniak A 2011 *Journal of Materials Science: Materials in Electronics* **22** 1321-9
[34]Ostfeld A E, Deckman I, Gaikwad A M, Lochner C M and Arias A C 2015 *Sci. Rep.* **5** 15959

[35]Cheng P L, Law T W, Liu C K, Chong I T and Lam D C C 2002 *2nd International IEEE Conference on Polymers and Adhesives in Microelectronics and Photonics.* 205-10
[36]Ha M, Zhang W, Braga D, Renn M J, Kim C H and Frisbie C D 2013 *ACS Appl. Mater. Interfaces* **5** 13198-206
[37]Kang B J, Lee C K and Oh J H 2012 *Microelectron. Eng.* **97** 251-4
[38]Correia V, Mitra K Y, Castro H, Rocha J G, Sowade E, Baumann R R and Lanceros-Mendez S 2018 *Journal of Manufacturing Processes* **31** 364-71
[39]Ionescu C, Svasta P, Vasile A and Bonfert D 2012 *2012 IEEE 18th International Symposium for Design and Technology in Electronic Packaging (SIITME)* 85-9
[40]Wang G, Tao X, Xin J H and Fei B 2009 *Nanoscale Res. Lett.* **4** 613-7
[41]Ouyang J, Chu C W, Chen F C, Xu Q and Yang Y 2005 *Adv. Funct. Mater.* **15** 203-8
[42]Chen B, Cui T, Liu Y and Varahramyan K 2003 *Solid·State Electron.* **47** 841-7
[43]Cui T, Liu Y, Chen B, Zhu M and Varahramyan K 2005 *Solid·State Electron.* **49** 853-9
[44]Liu Y, Cui T and Varahramyan K 2003 *Solid·State Electron.* **47** 1543-8
[45]Castro H F, Correia V, Sowade E, Mitra K Y, Rocha J G, Baumann R R and Lanceros-Méndez S 2016 *Org. Electron.* **38** 205-12
[46]Walker S B and Lewis J A 2012 *J. Am. Chem. Soc.* **134** 1419-21
[47]Ouyang J, Xu Q, Chu C-W, Yang Y, Li G and Shinar J 2004 *Polymer* **45** 8443-50
[48]Xing R, Wang S, Zhang B, Yu X, Ding J, Wang L and Han Y 2017 *RSC Adv.* **7** 7725-33
[49]Tang B, White S P, Frisbie C D and Lodge T P 2015 *Macromolecules* **48** 4942-50
[50]Cho J H, Lee J, Xia Y, Kim B, He Y, Renn M J, Lodge T P and Frisbie C D 2008 *Nat. Mater.* **7** 900-6
[51]Horowitz P and Hill W 1989 *The Art of Electronics* (New York, NY: New York, NY : Cambridge University Press)